molbank

MDPI

Communication

Synthesis of a Stable Long-Wavelength Fluorescent BODIPY FL-NAADP Conjugate

Zhong Guan [1] and James T. Slama [2,*]

[1] Department of Medicinal and Biological Chemistry, University of Toledo, Toledo, OH 43614, USA; zhong.guan@utoledo.edu
[2] Department of Medicinal and Biological Chemistry, College of Pharmacy and Pharmaceutical Sciences, University of Toledo, 3000 Arlington Avenue, Toledo, OH 43614, USA
* Correspondence: james.slama@utoledo.edu; Tel.: +1-419-383-1925

Abstract

Nicotinic acid adenine dinucleotide phosphate (NAADP) is a second messenger that stimulates intracellular Ca^{2+} release in both mammalian cells and echinoderm egg homogenates. A NAADP linked covalently to a stable long-wavelength fluorescent dye would be a useful probe with which to characterize NAADP–receptor interactions in solution and potentially to determine intracellular-binding localization. We report the synthesis of a BODIPY-NAADP covalent conjugate made through linking the carboxyl group of BODIPY FL to the primary amino group of 5-(3-aminopropyl)-NAADP through amide bond formation. The starting pyridine dinucleotide analog, 5-(3-aminopropyl)-NAADP was available through enzyme-catalyzed base exchange between NADP and a substituted nicotinic acid analog. The resulting 5-BODIPY-NAADP conjugate was purified to homogeneity using ion-exchange chromatography, was produced in milligram quantities, and its spectroscopic properties were characterized.

Keywords: nicotinic acid adenine dinucleotide phosphate (NAADP); Ca^{2+} signaling; fluorescent dinucleotide; pyridine dinucleotide; chemoenzymatic synthesis

check for updates

Academic Editor: Fawaz Aldabbagh

Received: 5 August 2025
Revised: 22 October 2025
Accepted: 30 October 2025
Published: 5 November 2025

Citation: Guan, Z.; Slama, J.T. Synthesis of a Stable Long-Wavelength Fluorescent BODIPY FL-NAADP Conjugate. *Molbank* **2025**, *2025*, M2085. https://doi.org/10.3390/M2085

Copyright: © 2025 by the authors. Licensee MDPI, Basel, Switzerland. This article is an open access article distributed under the terms and conditions of the Creative Commons Attribution (CC BY) license (https://creativecommons.org/licenses/by/4.0/).

1. Introduction

Nicotinic acid adenine dinucleotide phosphate (NAADP, Figure 1) is a Ca^{2+}-mobilizing intracellular second messenger active in echinoderms, plants, and human tissues [1]. In cultured human cells, NAADP releases Ca^{2+} from endosomal- and lysosomal-localized calcium stores through the activation of two-pore channels (TPCs) [2]. NAADP TPC activation is mediated through the intermediacy of two different 23–24 kDa NAADP-binding proteins, JPT2 [3,4] and LSM12 [5], which specifically bind the dinucleotide at micromolar concentrations and activate TPCs through protein–protein interaction. NAADP-mediated Ca^{2+} release has been shown to be of importance both in viral infections and cancer [6].

NAADP itself [7], and a variety of substituted NAADP analogs, have been prepared using enzyme-catalyzed pyridine base-exchange reactions and tested for the ability to induce Ca^{2+} release in sea urchin egg homogenates and in cultured human cells [8–10]. Chemoenzymataic synthesis has resulted in the production of important NAADP derivatives including membrane-permeant analogs [11,12] and light-activatable caged derivatives [13,14]. However, except for the short-wavelength etheno-NAADP analogs [15], fluorescent NAADP conjugates have not been developed. Long-wavelength fluorescent

NAADP analogs would constitute a class of biological probes that would be useful tools to advance studies of NAADP-mediated signaling. Fluorescent NAADP conjugates would permit the development of competition ligand-binding assays using fluorescence or fluorescence depolarization, could identify intracellular locations of NAADP binding, and facilitate biophysical studies of NAADP-binding protein interactions.

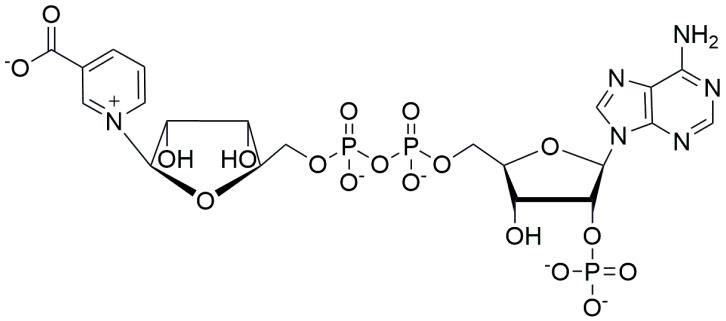


Figure 1. The structure of NAADP.

In this report, we describe linking the amino group of 5-(3-aminopropyl)-NAADP (**1**) to the *N*-hydroxysuccinimide ester of BODIPY FL (**2**), resulting in the formation of an amide bond and synthesis of BODIPY FL-NAADP (**3**) (Figure 2). BODIPY FL offers a well characterized fluorophore with high quantum yield, excitation > 500 nm, emission at ~520 nm, and high photochemical stability [16]. BODIPY conjugates of bio-active molecules including alkaloids [17,18] and terpenes [19] have recently been reported as biochemical probes.

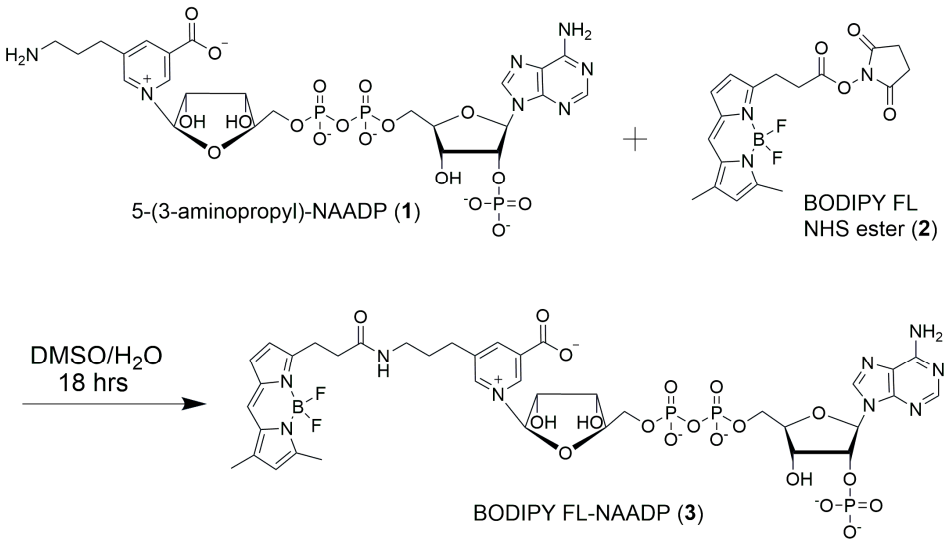


Figure 2. Synthesis of BODIPY FL-NAADP (**3**) from 5-(3-aminopropyl)-NAADP (**1**) and BODIPY FL *N*-hydroxysuccinimide ester (**2**).

2. Results and Discussion

2.1. Synthesis of **3**

The starting materials for this synthesis were 5-(3-aminopropyl)-NAADP (**1**) and BODIPY FL *N*-hydroxysuccinimide ester (**2**) (Figure 2). Dinucleotide **1** was previously synthesized and characterized as the product from the enzyme-catalyzed pyridine base-exchange reaction between NADP and 5-(3-aminopropyl)-nicotinic acid [10]. Compound **2** was available commercially or could be produced in high yield in a single step from BODIPY FL and *N*-hydroxysuccinimide (NHS).

Active ester **2** was directly coupled with dinucleotide **1** by forming an amide linkage. To obtain the best result, a highly concentrated solution of **1** and **2** must be produced. One equivalent of compound **1** was reacted with six equivalents of compound **2** in a 2:1 DMSO/water solution for 18 h at ambient temperature.

The product **3** was purified by anion-exchange chromatography using a stationary phase of DEAE-cellulose and a mobile phase consisting of a linear gradient formed between water and 0.4 M ammonium bicarbonate [10]. The eluted fractions which contained **3** were identified by their UV absorption, combined, and lyophilized to yield NAADP-BODIPY dye conjugate **3** as its ammonium salt.

2.2. Spectroscopic Properties of **3**

NAADP-BODIPY dye conjugate **3** was characterized using ^{1}H- and ^{13}C-NMR spectra, its UV/visible spectrum, and mass spectrometry.

The ^{1}H-NMR spectrum of **3** exhibits five low-field singlets from the aromatic purine and nicotinamide rings (δ 8–9 ppm), signals from the aromatic hydrogens of the BODIPY moiety (δ 6–7 ppm), a distinctive set of doublets from the anomeric carbons of the ribose rings (δ 6.06 and 6.02 ppm), and two high-field methyl signals from the BODIPY methyl groups (δ 2.39 and 2.07). The ribosyl protons and the four linking methylene groups form a complex set of overlapping high-field signals between 1.5 and 4.5 ppm (Figure S1).

The UV/visible spectrum combines the chromophores of the two component parts (Figure 3) with maxima at 261 nm and 506 nm. Fluorescence excitation spectrum recorded in PBS at pH 7.4 shows a peak absorption at 505 nm and a peak emission at 520 nm.

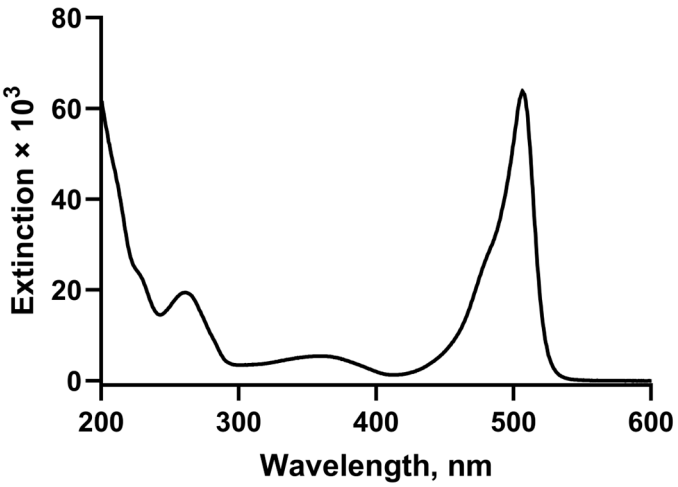


Figure 3. Electronic absorption spectrum of BODIPY FL-NAADP (**3**).

3. Materials and Methods

3.1. General Procedures

Reagents and anhydrous solvents were purchased from Millipore Sigma (Burlington, MA, USA) or Thermo Scientific Chemicals (Thermo Fisher Scientific Inc., Waltham, MA, USA) and were used without purification unless stated otherwise. ACS Reagent-grade solvents were purchased from Thermo Fisher Scientific (Waltham, MA, USA). All reactions were conducted in washed and oven-dried glassware (120 °C).

The proton (^{1}H) NMR and the carbon (^{13}C) NMR spectra were recorded at 14.0954 Tesla (^{1}H Larmor frequency of 600 MHz and ^{13}C Larmor Frequency of 150.903 MHz), using the Bruker Avance NMR with Cryoprobe (Bruker Corp., Billerica, MA, USA) or Varian Inova 600 MHz spectrometers (Palo Alto, CA, USA). Chemical shifts are reported in parts per

million (ppm, δ) and referenced to the residual proton signal of the deuterated solvent (^{1}H, at δ 4.70, D_2O), or an internal standard of tetramethylsilane (TMS) when $CDCl_3$ was used.

3.2. Preparative Anion-Exchange HPLC

Anion-exchange chromatography was performed using a Bio-Rad BioLogic Duo Flow™ chromatography system equipped with a 260 nm UV detector. The stationary phase was AG MP-1 (200–400 mesh) anion-exchange resin trifluoroacetate form (Bio-Rad Laboratories, Hercules, CA, USA) packed into heavy walled glass columns (1 × 17 cm). The mobile phase was a linear gradient formed by mixing deionized water (solvent A) and 150 mM aqueous TFA (solvent B) [20]. A 5 mL injection loop was fitted to the HPLC system, and the flow rate was 6 mL/min throughout the purification. The chromatography was developed as follows: (1) 6 mL solvent A was applied through the injection loop; (2) 25 mL solvent A was applied through the column; (3) a linear gradient of TFA was formed over a total volume of 185–400 mL; (4) 40 mL solvent B was applied to clean the column; and (5) 40 mL solvent A was applied to re-equilibrate the column.

3.3. MALDI Analysis

Super DHB (sDHB), 9:1 2,5-dihydroxybenzoic acid:2-hydroxy-5-methoxybenzoic acid, was purchased from Millipore Sigma (Burlington, MA, USA). A peptide Calibration Standard II and an MTP 384 Ground Steel TF target plate were purchased from Bruker (Billerica, MA, USA).

A matrix solution of sDHB was prepared (20 mg/mL) in 33% acetonitrile–water with 0.1% TFA (TA 33). The peptide calibration standard was prepared as directed by the supplier. Equal volumes of matrix and analyte solution (in TA 33) were premixed and 0.5 µL of the resulting solution was spotted onto the target plate. The prepared calibration solution was spotted on an adjacent spot of the target plate. MALDI spectra were collected in positive ion detection mode on a Bruker UltraFlextrem MALDI-TOF/TOF (Billerica, MA, USA). Instrument calibration with the peptide II standard provided a less than 5 ppm error.

3.4. Determination of UV/Visible Extinction Coefficients

Exact concentrations of dinucleotide **3** were determined by measurement of the quantity of organic phosphate according to the method of B. Ames, 1966 [21].

3.5. Analytical HPLC Ion-Exchange Chromatography

The analytical HPLC procedure described by Alexson et al., 1981 [20], was modified to accommodate the more hydrophobic BODIPY-containing dinucleotides. The stationary phase consisted of AG MP-1 (200–400 mesh) anion-exchange resin trifluoroacetate form (Bio-Rad Laboratories, Hercules, CA, USA) packed into heavy walled glass columns (6.6 mm × 10.5 cm). The mobile phase consisted of a linear gradient formed between 5% ethanol in water (A) and 0.15 M TFA with 20% ethanol in water (B). A flow rate of 1.5 mL/min was used and the effluent was monitored by measuring the UV absorption at 260 nm.

3.6. 5-(3-Aminopropyl)-NAADP (**1**)

5-(4-Aminopropyl)-nicotinic acid (CAS Registry # 1515508-35-6) (35 mg, 0.194 mmol) was dissolved in water (6 mL) and stirred for 30 min at 37 °C. After this time, the pH was adjusted to 7.5 with 1 M NaOH and stirred for 30 min. The pH was measured again and readjusted to pH = 7.5 with 1 M NaOH. This procedure was repeated until the pH was stabilized. After the pH had stabilized, NADP (15 mg, 0.018 mmol) was added and stirred for 5 min at 37 °C. Next, recombinant E98G *Aplysia californica* ADP-ribosyl cyclase [22,23] (180 µL, 36 ng) was added as the catalyst for the pyridine base-exchange reaction, and

the reaction was stirred at 37 °C for 6 h. At the end of 6 h, analysis by HPLC confirmed that the starting material (NADP) had been consumed. The sample was then injected onto the HPLC column, and the product was purified by anion-exchange chromatography in water/TFA gradients according to the HPLC method described in Section 3.2. The fractions showing UV absorption at 260 nm were combined and lyophilized. After the HPLC column, the combined product was extracted with 1:4 tri-*n*-octylamine/$CHCl_3$ with a 1:4 ratio of organic to aqueous phase. The phases were separated by centrifugation (using a clinical centrifuge with 50 mL Pyrex tubes), and the chloroform-rich organic phase was removed. The aqueous phase was frozen and lyophilized to give the product, a white amorphous solid, as a tri-*n*-octylamine salt. The spectroscopic properties of this material agreed with that which had been published previously [10], and it was used in the next step as the tri-*n*-octylammonium salt without further purification. Yields for this reaction were typically 30–60%.

3.7. BODIPY FL-NAADP (**3**)

One equivalent of compound **1** (4.12 mg, 0.00514 mmol) and 6 equivalents of compound **2** (12 mg, 0.03 mmol) were dissolved in a solution of 0.5 mL DMSO and 0.25 mL H_2O in a 1.5 mL Eppendorf tube, and the mixture was stirred at ambient temperature. After 18 h, the reaction mixture was diluted with 1 mL of water, and then loaded onto a column of DEAE-cellulose (10 × 100 mm) (Whatman DE-53 cellulose #4058200). The separation was developed by applying a linear gradient formed between 500 mL of water and 500 mL of 400 mM NH_4HCO_3 and 10 mL fractions were collected. The effluent fractions were monitored for UV/visible absorption, and those showing UV absorption at both 260 nm and 506 nm were combined and lyophilized to give the red amorphous solid product as its ammonium salt. Based on the extinction coefficient of BODIPY FL at 506 nm, we isolated 2.2 mg (40% yield) of the product.

UV/visible electronic absorption spectrum (H_2O) exhibited peaks at λ_{max} 506 nm (ε_{506}, 63,800 L mol^{-1} cm^{-1}) and λ_{max} 261 nm (ε_{261}, 19,400 L mol^{-1} cm^{-1}) A_{506}/A_{261} = 3.29; fluorescence excitation spectrum (recorded in PBS at pH 7.4) maxima at 506 nm; fluorescence emission peak at 520 nm;

^{1}H-NMR (600 MHz, D_2O) (Figure S1) δ 8.97 (s, 1H), 8.85 (s, 1H), 8.53 (s, 1H), 8.30 (s, 1H), 7.99 (s, 1H), 6.92 (s, 1H, -H BODIPY), 6.88 (d, 1H, *J* = 3.96, -H BODIPY), 6.38 (d, 1H, *J* = 4.02, -H BODIPY), 6.10 (s, 1H, -H BODIPY), 6.06 (d, 1H, *J* = 5.34, -H anomeric), 6.02 (d, 1H, *J* = 5.58, -H anomeric), 4.92 (m, 1H), 4.56–4.17 (m, 9H), 3.27–3.10 (m, 4H), 2.69 (m, 2H), 2.52 (t, 2H, *J* = 8.22, -CH_2), 2.39 (s, 3H, -CH_3), 2.07 (s, 3H, -CH_3), 1.77 (m, 2H); Proton-decoupled ^{13}C-NMR (D_2O, 600 MHz) (Figure S2), δ 176.6, 175.0, 161.2, 155.8, 153.6, 150.1, 148.4, 146.3, 145.5, 143.9, 140.2, 139.5, 139.4, 136.4, 134.6, 132.6, 128.8, 123.8, 120.9, 118.2, 116.8, 99.7, 86.7, 86.2, 83.4, 77.4, 76.9, 70.4, 69.8, 65.3, 65.0, 38.4, 34.5, 28.9, 27.9, 24.5, 14.1, 10.4.

Positive mode MALDI mass spectra (Figure S3; Table S1): Calcd. *m*/*z* for $C_{38}H_{48}BF_2N_9O_{19}P_3$, $[M]^+$ 1076.2335; measured *m*/*z* was 1076.2350 (1.39 ppm error).

Subsequent to our original purification, we found that preparative chromatography using DEAE-Sephacel worked as well as the Whatman DE-53 cellulose. An example of the DEAE-Sephacel chromatography is presented in the Supplementary Materials as Figure S4 (page 10). The purity of the product was determined to be >92% using analytical HPLC anion-exchange chromatography. The chromatographic profile is available as Figure S5 (page 11) in the Supplementary Materials.

Supplementary Materials: The following supporting information can be downloaded at: Figure S1. ^{1}H NMR (600 MHz) of BODIPY FL-NAADP (**3**). Figure S2. Proton-decoupled ^{13}C NMR (151 MHz) of BODIPY FL-NAADP (**3**). Figure S3. MALDI mass spectrum of BODIPY FL-NAADP (**3**). Table S1.

Mass list from MALDI measurement. Figure S4. Preparative DEAE anion-exchange chromatography of BODIPY FL-NAADP (**3**). Figure S5. Anion-exchange HPLC trace for BODIPY FL-NAADP (**3**).

Author Contributions: Conceptualization, J.T.S. and Z.G.; methodology, Z.G.; writing—original draft preparation, Z.G.; writing—review and editing, J.T.S.; funding acquisition, J.T.S. All authors have read and agreed to the published version of the manuscript.

Funding: This research was funded by the National Institutes of Health, grant number GM 088790.

Data Availability Statement: All relevant data can be found in the Supplementary Materials.

Acknowledgments: We wish to thank Christopher G. Gianopoulos and the Instrumentation Center, College of Natural Sciences and Mathematics, University of Toledo, for obtaining the high-resolution MALDI mass spectra.

Conflicts of Interest: The authors declare no conflicts of interest.

Abbreviations

The following abbreviations are used in this manuscript:

DEAE-cellulose	Diethylaminoethyl-substituted cellulose for anion exchange
DHB	Dihydroxybenzoate
BODIPY FL	Refers to CAS registry # 165599-63-3
DMSO	Dimethyl sulfoxide
NAADP	Nicotinic acid adenine dinucleotide phosphate
NADP	Nicotinamide adenine dinucleotide phosphate
NHS	*N*-hydroxysuccinimide
PBS	Phosphate-buffered saline solution
TFA	Trifluoroacetic acid
TPCs	Two-pore channels

References

1. Galione, A. A primer of NAADP-mediated $Ca^{(2+)}$ signalling: From sea urchin eggs to mammalian cells. *Cell Calcium* **2015**, *58*, 27–47. [CrossRef] [PubMed]
2. Patel, S. Function and dysfunction of two-pore channels. *Sci. Signal.* **2015**, *8*, re7. [CrossRef] [PubMed]
3. Gunaratne, G.S.; Brailoiu, E.; He, S.; Unterwald, E.M.; Patel, S.; Slama, J.T.; Walseth, T.F.; Marchant, J.S. Essential requirement for JPT2 in NAADP-evoked $Ca^{(2+)}$ signaling. *Sci. Signal.* **2021**, *14*, eabd5605. [CrossRef] [PubMed]
4. Roggenkamp, H.G.; Khansahib, I.; Hernandz, C.; Zhang, Y.; Lodygin, D.; Krüger, A.; Gu, F.; Möckl, F.; Löhndorf, A.; Wolters, V.; et al. HN1L/JPT2: A signaling protein that connects NAADP generation to Ca^{2+} microdomain formation. *Sci. Signal.* **2021**, *14*, eabd5647. [CrossRef]
5. Zhang, J.; Guan, X.; Shah, K.; Yan, J. Lsm12 is an NAADP receptor and a two-pore channel regulatory protein required for calcium mobilization from acidic organelles. *Nat. Commun.* **2021**, *12*, 4739. [CrossRef]
6. Marchant, J.S.; Gunaratne, G.S.; Cai, X.; Slama, J.T.; Patel, S. NAADP-binding proteins find their identity. *Trends Biochem. Sci.* **2022**, *47*, 235–249. [CrossRef]
7. Bernofsky, C. Nicotinic Acid Adenine Dinucleotide Phosphate ($NAADP^+$). *Methods Enzym.* **1980**, *66*, 105–112.
8. Jain, P.; Slama, J.T.; Perez-Haddock, L.A.; Walseth, T.F. Nicotinic acid adenine dinucleotide phosphate analogues containing substituted nicotinic acid: Effect of modification on $Ca^{(2+)}$ release. *J. Med. Chem.* **2010**, *53*, 7599–7612. [CrossRef]
9. Lee, H.C.; Aarhus, R. Structural determinants of nicotinic acid adenine dinucleotide phosphate important for its calcium-mobilizing activity. *J. Biol. Chem.* **1997**, *272*, 20378–20383. [CrossRef]
10. Trabbic, C.J.; Zhang, F.; Walseth, T.F.; Slama, J.T. Nicotinic acid adenine dinucleotide phosphate analogues substituted on the nicotinic acid and adenine ribosides. effects on receptor mediated Ca^{2+} release. *J. Med. Chem.* **2015**, *58*, 3593–3610. [CrossRef]
11. Krukenberg, S.; Möckl, F.; Weiß, M.; Dekiert, P.; Hofmann, M.; Gerlach, F.; Winterberg, K.J.; Kovacevic, D.; Khansahib, I.; Troost, B. MASTER-NAADP: A membrane permeable precursor of the Ca^{2+} mobilizing second messenger NAADP. *Nat. Commun.* **2024**, *15*, 8008. [CrossRef]
12. Parkesh, R.; Lewis, A.M.; Aley, P.K.; Arredouani, A.; Rossi, S.; Tavares, R.; Vasudevan, S.R.; Rosen, D.; Galione, A.; Dowden, J. Cell-permeant NAADP: A novel chemical tool enabling the study of Ca^{2+} signalling in intact cells. *Cell Calcium* **2008**, *43*, 531–538. [CrossRef]

13. Lee, H.C.; Aarhus, R.; Gee, K.R.; Kestner, T. Caged nicotinic acid adenine dinucleotide phosphate: Synthesis and use. *J. Biol. Chem.* **1997**, *272*, 4172–4178. [CrossRef]
14. Parkesh, R.; Vasudevan, S.R.; Berry, A.; Galione, A.; Dowden, J.; Churchill, G.C. Chemo-enzymatic synthesis and biological evaluation of photolabile nicotinic acid adenine dinuclotide phosphate ($NAADP^+$). *Org. Biomol. Chem.* **2007**, *5*, 441–443. [CrossRef] [PubMed]
15. Lee, H.C.; Aarhus, R. Fluorescent analogs of NAADP with calcium mobilizing activity. *Biochim. Biophys. Acta* **1998**, *1425*, 263–271. [CrossRef] [PubMed]
16. Loudet, A.; Burgess, K. BODIPY dyes and their derivatives: Syntheses and spectroscopic properties. *Chem. Rev.* **2007**, *107*, 4891–4932. [CrossRef] [PubMed]
17. Jurášek, M.; Dráberová, E.; Řehulka, J.; Gurská, S.; Ivanova, A.; Polishchuk, P.; Ječmeňová, K.; Fähnrich, J.; Marešová, A.; Tauchen, J.; et al. Colchicine-BODIPY Probes: Evidence for the Involvement of Intracellular Membranes in the Targeting of Colchicine to Tubulin. *ACS Pharmacol. Transl. Sci.* **2025**, *8*, 1965–1985. [CrossRef]
18. Lin, W.; Liu, J.; Jeffries, C.; Yang, L.; Lu, Y.; Lee, R.E.; Chen, T. Development of BODIPY FL vindoline as a novel and high-affinity pregnane X receptor fluorescent probe. *Bioconjugate Chem.* **2014**, *25*, 1664–1677. [CrossRef]
19. Stanková, J.; Jurasek, M.; Hajduch, M.; Dzubak, P. Terpenes and Terpenoids conjugated with BODIPYs: An overview of biological and chemical properties. *J. Nat. Prod.* **2024**, *87*, 1306–1319. [CrossRef]
20. Alexson, J.T.; Bodley, J.W.; Walseth, T.F. A volatile liquid chromatography system for nucleotides. *Anal. Biochem.* **1981**, *116*, 347–360. [CrossRef]
21. Ames, B.N. Assay of inorganic phosphate, total phosphate and phosphatases. *Methods Enzym.* **1966**, *8*, 115–118. [CrossRef]
22. Graeff, R.; Liu, Q.; Kriksunov, I.A.; Hao, Q.; Lee, H.C. Acidic residues at the active sites of CD38 and ADP-ribosyl cyclase determine nicotinic acid adenine dinucleotide phosphate (NAADP) synthesis and hydrolysis activities. *J. Biol. Chem.* **2006**, *281*, 28951–28957. [CrossRef] [PubMed]
23. Munshi, C.; Lee, H.C. High-Level Expression of Recombinant *Aplysia* ADP-Ribosyl Cyclase in *Pichia pastoris* by Fermentation. *Protein Expr. Purif.* **1997**, *11*, 104–110. [CrossRef] [PubMed]

Disclaimer/Publisher's Note: The statements, opinions and data contained in all publications are solely those of the individual author(s) and contributor(s) and not of MDPI and/or the editor(s). MDPI and/or the editor(s) disclaim responsibility for any injury to people or property resulting from any ideas, methods, instructions or products referred to in the content.